HHS Public Access

Author manuscript

NanoImpact. Author manuscript; available in PMC 2021 January 01.

Published in final edited form as:

NanoImpact. 2020 January ; 17: . doi:10.1016/j.impact.2019.100202.

Evaluation of the cytotoxic and cellular proteome impacts of food-grade TiO_2 (E171) using simulated gastrointestinal digestions and a tri-culture small intestinal epithelial model

Xiaoqiong Cao[a,1], **Tong Zhang**[b,1], **Glen M. DeLoid**[a], **Matthew J Gaffrey**[b], **Karl K. Weitz**[b], **Brian D. Thrall**[b], **Wei-Jun Qian**[b,*], **Philip Demokritou**[a,*]

[a]Center for Nanotechnology and Nanotoxicology, Department of Environmental Health, Harvard T. H. Chan School of Public Health, Boston, MA 02115, USA

[b]Biological Sciences Division, Pacific Northwest National Laboratory, Richland, WA, USA

Abstract

Engineered nanomaterials (ENMs) are widely used in the food industry; however, regulations for ENMs in food are still in the early stages of development due to insufficient health data. This study investigated the cytotoxicity and changes to the proteomic profile in an *in vitro* small intestinal epithelium model after exposure to digested food models containing the ubiquitous engineered particulate food additive, TiO_2 (E171) with an average size around 110 nm. TiO_2 at 0.75% or 1.5% (w/w) concentrations in either a fasting food model (FFM) or a standardized food model (SFM) based on American diet were digested using an *in vitro* oral-gastric-small intestinal simulator, and the resulting digestas were applied to a small intestinal epithelium tri-culture cellular model. Effects on cell layer integrity, cytotoxicity, and oxidative stress were assessed. In order to explore the impact on cellular processes beyond basic cytotoxicity, mass spectrometry-based quantitative proteomic analyses of control and exposed tri-culture cells was performed. TiO_2 in FFM, but not in SFM, produced significant, dose-dependent cytotoxicity (24%, $p<0.001$), and at the higher dose caused significant oxidative stress (1.24-fold, $p<0.01$), indicative of a food matrix effect. No significant perturbations of the cellular proteome were observed with TiO_2 in either FFM or SFM food models. However, proteins involved in energy metabolism and protein synthesis were up-regulated by digestas from SFM compared to those from FFM, indicative of a food matrix effect on the cellular proteome. Interestingly, the differences in profiles between the two food models was more pronounced in the presence of TiO_2. Together, these results indicate that TiO_2 in a fasting diet may be slightly cytotoxic, and that ingested TiO_2 does not significantly alter the epithelial proteome, whereas the food matrix alone can have a dramatic effect on the proteome.

*corresponding authors Philip Demokritou, pdemokri@hsph.harvard.edu, Wei-Jun Qian, weijun.qian@pnnl.gov.

[1]These authors contributed equally to the present work.

Conflicts of interest

There are no conflicts to declare.

Keywords

Engineered Nanomaterials; Food additive; Titanium Dioxide; Toxicity; Proteomics

Introduction

Nanotechnology has been rapidly developing over the past two decades. The unusual properties of engineered nanomaterials (ENMs) make them particularly useful in the food industry, where ENMs are widely used to improve food quality, safety, and nutritional benefits [1–8]. In some cases, ENMs are added to food products intentionally, such as when ENMs are used to modify color and rheology, or as delivery systems. In other cases, ENMs are not added to the food directly, but may find their way into the final food products through contact with other materials containing ENMs, (*i.e.*, ENMs used for food packaging and sensors) or in agriculture applications [9]. With the increasing number of novel applications, and a growing number of ENMs with potential uses in the agriculture and food industries, human exposures are inevitable [10].

The growing human oral exposure to expanding libraries of inorganic and organic ENMs raises concerns about the potential health risks [11–13]. Emerging nano-safety research shows that the smaller size of the nano-scale materials gives them unique physicochemical properties, including much larger surface-to-mass ratios compared to bulk or micron-scale materials, which renders them more bioactive [12,14,15]. More importantly, it was shown that nanoscale materials can bypass biological barriers and become systemic and interfere with cellular processes and functions [16–20].

In addition, interactions of ENMs with complex food matrices, and their transformations across the gastrointestinal tract (GIT) may alter an ENM's properties, such as electrical charge, solubility, agglomeration state, and surface composition [1,21–23]. As a result, the biological fate and potential toxicity of ingested ENMs may be considerably different from those of the pristine ENMs. Therefore, understanding and accounting for these transformations is essential to the study of ingested ENMs [13,21]. Nonetheless, the majority of *in vitro* cell culture studies of ingested ENMs have ignored the impact of food matrix and GIT bio-transformations [24].

The widely used food additive titanium dioxide (TiO_2), known as E171, is used as a whitening agent in over 900 food products, such as chewing gums, dairy products, and sweets [25,26]. The human exposure to TiO_2 through oral ingestion has been estimated to be about 1 mg of Ti /kg body weight/day for US adults, and between 2 and 4 times that amount for US children [26]. Food-grade TiO_2 (E171) has a wide range of particle sizes. It has been reported that about 40% of the particles in food-grade TiO_2 are in the nanoscale (are smaller than 100 nm in at least one dimension) [26–28].

Results from in-vitro cellular and animal studies on the oral toxicity, and tissue accumulation of TiO_2 continue to grow and are contradictory [28,29]. This is likely because the different studies used different oral doses, particle sizes and crystal forms. For example, a single oral dose of TiO_2 nanoparticles (25, 80, or 155 nm at 5000 mg/kg bw) induced

hepatic injury, nephrotoxicity, and myocardial damage, and also resulted in TiO_2 accumulation in liver, lung, spleen, and kidney tissues of mice [30]. In contrast, in a chronic study in which rats received repeated doses of up to 1041 mg/kg of 21 nm mixed anatase/rutile TiO_2 nanoparticles, no significant toxicity or accumulation in tissues or urine was observed, and high concentrations of TiO_2 were detected in feces, suggesting elimination primarily by the fecal route [31]. Due to growing concerns about the safety of E171, the French food safety authority has recently decided to ban foods containing E171 from their markets beginning January 1, 2020. However, US regulations pertaining to TiO_2 and other ENMs in food products are still in the early stages of development, largely due to a lack of relevant health data. [23,32]

In this *in vitro* study, TiO_2 (E171) was incorporated into either a fasting food model (FFM) or a standardized food model (SFM) based on the typical American diet [33]. The food models, with or without TiO_2, were digested using a three phase (oral, gastric, small intestinal) GIT simulator, and the resulting digesta was applied to an *in vitro* small intestinal epithelial tri-culture cellular model for toxicity assessments [21]. It is worth noting that this integrated methodology takes into account the effects of the food matrix and transformations of ENMs across the GIT [21]. Liquid chromatography coupled with tandem mass spectrometry (LC-MS/MS) was employed to determine the cellular proteome response to ingested TiO_2. A highly reproducible proteomic workflow with label-free quantification made it possible to quantitatively profile the potential alterations of the proteomes of the gut tri-culture cellular system. This study adds important information to the knowledge of the potential impacts of ingested nanomaterials under physiologically relevant conditions.

Materials and Methods

Materials

Food-grade TiO_2 (E171) was purchased from Pronto Foods Co. (Chicago, IL, USA). Detailed physico-chemical characterization of the TiO_2 (E171) was performed and described in detail by the authors in previous publication [27,28]. Based on Title 21 of Code of the Federal Regulations (21 CFR §73.575), the allowable maximum concentrations of the color additive TiO_2 (E171) is 1% by weight, of the food. Therefore, two starting concentrations of food-grade TiO_2 (E171) were chosen for this study, 0.75% and 1.5% w/w in food models. Assuming average human food intake is 2.5 kg per day and average human body weight is 75 kg, the doses used in this study is equal to 150 and 300 mg Ti/kg body weight/day.

Food models

Phosphate buffer (5 mM) at pH 7.0 was used as a fasting food model (FFM). The standardized food model (SFM), based on the typical American diet, was previously described by the authors [33]. In summary, SFM is prepared as an oil-in-water emulsion consisting of 5.2% digestible carbohydrate (modified corn starch), 4.6% sugar (sucrose), 3.4% protein (sodium caseinate), 3.4% fat (corn oil), 0.7% dietary fiber (pectin), and 0.5% sodium chloride, and spray-dried to produce a powder for storage at 4 °C. To reconstitute 100 g of the SFM, 17.8 g of the powder was combined with 82.2 g distilled water and stirred at 900 RPM for 30 minutes.

Colloidal characterization before digestion and in small intestinal phase digesta

A laser diffraction particle size analyzer (Mastersizer 3000, Malvern Instruments, Ltd) was used to obtain the surface-weighted mean diameters (*D[3,2]*), volume-weighted mean diameters (*D[4,3]*), and volume-weighted size distributions of particles before digestion and in small intestinal phase digesta from the simulated GIT digestion (described below). Zeta-potential (ζ) were determined using a Zetasizer Nano-ZS (Malvern Instruments, Ltd., Worcestershire, UK). All measurements were performed in triplicate, at 25 °C, using disposable optical polystyrene micro-cuvettes.

In vitro simulated digestions

FFM and SFM alone (control, 0% TiO_2) or FFM and SFM containing 0.75% or 1.5% w/w TiO_2 (E171), were used as initial food inputs for simulated digestions. Six samples were generated in total, *as follows:* (1) FFM control (5 mM phosphate buffer alone); (2) FFM with TiO_2 (0.75% w/w); (3) FFM with TiO_2 (1.5% w/w); (4) SFM control; (5) SFM with TiO_2 (0.75% w/w); (6) SFM with TiO_2 (1.5% w/w).

In vitro simulated digestion of the above samples was performed using a 3-phase (oral, gastric, small intestinal) simulator (Figure 1) as previously described in detail by the authors [21]. Briefly, in the oral phase, food inputs were brought to 37 °C, mixed with pre-warmed (37 °C) simulated saliva fluid, and inverted by hand for 10 seconds to mimic agitation in the mouth. The resulting oral phase digestas were then combined with pre-warmed simulated gastric fluid and incubated at 37 °C for two hours in a shaking incubator at 200 RPM to complete the stomach phase. In the small intestinal phase, stomach digestas were combined with pre-warmed solutions containing additional salts, bile extract and lipase to simulate intestinal fluid, and incubated at 37 °C for 2 hours, while maintaining a constant pH of 7.0, using a pH stat titration device (TitroLine® 7000, SI Analytics, GmbH, Germany).

It is worth noting that the initial concentrations of TiO_2 (E171) were diluted by a factor of 1/48 in total with digestive fluids in the oral (1/2), gastric (1/2) and small intestinal (1/3) phases, and with cell culture medium (1/4) before being applied to cells. Therefore, the final concentrations of TiO_2 (E171) used to expose the triculture cellular model were 150 μg/mL and 300 μg/mL for TiO_2 (E171) at starting concentrations of 0.75% and 1.5% w/w in food model, respectively.

Tri-culture small intestinal epithelial model and treatments

The tri-culture small intestinal epithelial model illustrated in Figure 1, was previously described and characterized in detail by the authors [21,43]. In summary, Caco-2 cells and HT29-MTX cells were first co-cultured for 2 weeks on an 0.4 μm pore membrane transwell insert in a 6-well cell culture plate, during which time the Caco-2 cells differentiate to resemble intestinal enterocytes, and HT29-MTX cells, similar to intestinal goblet cells, secrete large amounts of mucus. Raji B cells were then introduced to the basolateral compartment of the transwell plate to stimulate some of the matured Caco-2 cells to differentiate and acquire an M-cell-like phenotype. This tri-culture model of intestinal epithelium mimics the absorptive enterocytes, goblet cells and M cells that populate the

human small-intestinal lining and is therefore a suitable *in vitro* cell model for prediction of small intestinal toxicity in humans.

Cells were obtained from Sigma, Inc. Briefly, Caco-2 and HT29-MTX cells were grown in high-glucose DMEM supplemented with 10% heat-inactivated fetal bovine serum (FBS). Raji B cells were cultured in RPMI 1640 media supplemented with 10% FBS. For transwell inserts, Caco-2 and HT29-MTX cells were combined in a ratio of 3:1 (Caco-2 :HT29-MTX). 1.5 mL portion of the cell mixture was seeded in the apical chamber, and 2.5 mL of complete DMEM media was added to the basolateral compartment of a 6-well transwell plate. After four days, media was changed every other day, until day 15. On day 15 and 16, the media in the basolateral compartment was replaced with 2.5 mL of a suspension of Raji B cells at a concentration of 1×10^6 cells/mL in 1:1 DMEM: RPMI complete media. Cell layer integrity, cytotoxicity (LDH release), and proteomic analysis using tri-cultures on transwells were initiated on day 17.

Co-cultures of Caco-2/HT29-MTX in 96-well plates were used for oxidative stress (ROS production) studies (see below) which require closed-bottom adherent cell cultures suitable for plate reader fluorescence measurements. Raji B cells were not used here, since they are suspension feeder cells (not part of the epithelium) which were added to the transwell basolateral compartments to promote M-cell differentiation of some apical Caco-2 cells. Raji cells could adhere to mucus, or become incorporated in the epithelial layer, if applied apically in closed 96-well plates. To prepare co-cultures, Caco-2 and HT29-MTX cells at a 3:1 ratio was seeded at a total 3×10^4 cells/well (100 μL of cell mixture) in black-walled, clear optical bottom plates (BD Biosciences). After four days, media was changed every other day, until day 17.

The final small intestinal phase digestas from simulated digestions were combined with DMEM media at a ratio of 1:3, and the mixtures were applied to the cells on day 17 (1.5 mL to the apical compartment for transwell inserts, 200 μL per well for 96-well plates).

TEER, oxidative stress and cytotoxicity analysis

Transepithelial electrical resistance (TEER) was measured after 24 h treatment in transwell plate using an EVOM2 Epithelial Volt/Ohm Meter with a Chopstick Electrode Set (World Precision Instruments).

Cytotoxicity test was performed after 24 h treatment in transwell tri-cultures using the Pierce LDH assay kit (Sigma Aldrich, St. Louis, MO, USA) according to manufacturer's instructions. Briefly, untreated wells were used to measure spontaneous LDH release control. Lysed wells were used to measure maximum LDH release control. Apical fluid in each well was transferred to a tube which was then centrifuged, and 50 μL of the supernatant from each tube was dispensed in a fresh 96-well plate. 50 μL of reaction mixture was added. Plates were incubated at room temperature for 30 minutes, and 50 μL stop solution was added and mixed by tapping. Absorbance was measured at 490 nm (A_{490}) and 680 nm (A_{680}). To calculate LDH activity, A_{680} values were subtracted from measured A_{490} values to correct for instrument background. To correct for digesta background, LDH activities from no-cell controls were subtracted from test well LDH activities. Percent cytotoxicity

was calculated by subtracting spontaneous LDH release values from treatment values, dividing by total LDH activity (Maximum LDH activity – Spontaneous LDH activity), and multiplying by 100.

ROS analysis was performed after 6 h treatment in 96-well co-cultures. Production of ROS was assessed using the CellROX® green regent (Thermo Fisher Scientific, Waltham, MA, USA) according to manufacturer's instructions. Cells treated with 100 μM menadione for 1 h at 37°C were used as positive controls. Briefly, media was removed from test wells and replaced with 100 μL of working solution, and plates were incubated for 30 minutes at 37 °C. Wells were then washed 3 times with PBS, and fluorescence was measured at 480 nm (excitation)/520 nm (emission).

Sample preparation for proteomics

Cells were removed from transwell membrane using a cell scraper, and then lysed in 100 μl of lysis buffer (8 M urea in 50 mM NH_4HCO_3, pH 7.8) with sonication for 30s (Branson 1500R, Bransonic) and vortexing. Total solubilized proteins in the lysates was quantified using the Bicinchoninic acid (BCA) assay (Thermo Fisher Scientific). An aliquot of 300 μg of proteins was taken from each sample, and the sample volume was adjusted to 100 μl with lysis buffer. Reduction of proteins was carried out by incubation with 5 mM dithiothreitol (DTT) at 37 °C for 1h, followed by alkylation with 10 mM iodoacetamide at room temperature for 1 h in the dark. The resulting samples were diluted five-fold with 50 mM NH_4HCO_3, pH 7.8, and were then subjected to overnight digestion with sequencing grade modified trypsin (Promega) at a 1:50 enzyme to protein ratio in the presence of 1 mM $CaCl_2$ at 37 °C. Protein digests were further purified using solid phase extraction with Discovery C18 columns (Sigma-Aldrich). Prior to LC-MS/MS analysis, the peptides were resolubilized in 0.1% formic acid, quantified by BCA, and adjusted to a concentration of 0.1 μg/μl.

LC-MS/MS proteomic analysis

LC-MS/MS data were acquired on a Q-Exactive mass spectrometer (Thermo Scientific) coupled with a nanoAcquity UPLC system (Waters). Seven μL of peptide samples were injected and separated by a custom packed analytical C18 column (70 cm × 75 μm i.d., 3 um particle size of Jupiter C18, Phenomenex) in a 3 h gradient. The flow rate of the mobile phase (buffer A: 0.1% formic acid in water; buffer B: 0.1% formic acid in acetonitrile) was 300 nL/min. For peptide elution buffer B was increased to 12% at 36 min, 30% at 135 min, 45% at 175 min and finally 95% at 180 min. A data-dependent acquisition method was applied, in which a full MS scan was followed by up to 12 data-dependent MS/MS scans of the most abundant peptide precursors. A dynamic exclusion of 30 s was implemented to prevent repeated sequencing of previously selected peptides. For MS scans (400–2000 m/z; resolution of 35000 at 400 m/z), the automatic gain control (AGC) was set to $3\text{-}e^6$ with the maximum injection time (IT) of 20 ms. An isolation window of 2 m/z in the quadrupole was used for selecting precursor ions, which were fragmented by higher-energy collisional dissociation (HCD) at a normalized collision energy of 35. For MS/MS scans (200–2000 m/z with first fixed mass of 100 m/z; resolution of 17500 at 400 m/z), the AGC was set to $1\text{-}e^5$ and maximum IT was 100 ms.

Proteomic data analysis

Raw MS/MS data files were processed with MaxQuant (version 1.6.1.0). The non-redundant human UniProt proteome database (with 20,198 protein entries as of the April 2017 release) was used for searching. The searching parameters included carbamidomethylation on cysteine residues as fixed modifications, and acetylation on the peptide N-terminal, as well as oxidation on methionine, as variable modifications. Trypsin was selected as the enzyme for digestion, and a maximum of two missed cleavages was allowed. Mass tolerances for the first peptide search and main peptide search were 20 and 4.5 ppm, respectively. Match tolerance for MS/MS was 0.5 Da. A decoy database approach was used to limit the false discovery rate (FDR) to less than 0.01 for peptide spectrum matches. Proteins were also identified at FDR less than 0.01 with at least one unique peptide. For relative quantification, the label-free quantification (LFQ) algorithm was used with the minimum LFQ ratio count of 2. The “match between runs” feature was enabled with a 0.7 min match time window.

The LFQ protein intensities obtained from MaxQuant were first log2 transformed. Proteins quantified in all samples were used for further analysis. For data visualization in a clustered heatmap, a median-centered normalization was performed by subtracting the protein abundance from the median for each protein. The R package “pheatmap” was used to perform clustering analysis (“complete” as the clustering method) and to generate the heatmap. For statistical analysis, the protein abundance data were subjected to two-sample t test in Perseus (version 1.6.1.1). Permutation-based FDR calculation was used to control false discoveries in multiple-hypothesis testing. Significant proteins were defined with FDR < 5% as a cutoff. Gene ontology analyses of the significant proteins were performed using DAVID (the database for annotation, visualization and integrated discovery, https://david.ncifcrf.gov/).

Statistical analysis

All experiments, with the exception of proteomics, were performed in triplicate. Four biological replicates were used in the proteomic study. Results of TEER, cytotoxicity and ROS generation studies were analyzed by one-way ANOVA with Dunnett’s multiple comparisons test.

Results

Detailed physicochemical characterization of TiO_2 (E171) was reported previously by the authors [27]. Briefly, XRD patterns revealed an anatase crystal form, with a mean particle size by TEM of 113.4 ± 37.2 nm. Approximately 40% of particles had at least one dimension <100 nm, in agreement with what has been reported by others [26].

The surface charges (ζ-potentials), average particle diameters, and particle size distributions of the standardized food model (SFM) alone, of both SFM and fasting food model (FFM) with TiO2, and of digestas of both food models with and without TiO2, are summarized in Table 1 and Figure 2. Because undigested FFM alone is a simple salt solution with no particles its colloidal properties were not assessed. Moreover, it should be understood that the results of these colloidal analyses represent a heterogeneous mixture of particles,

including a variety of agglomerated food and digestive proteins, and lipid droplets in the case of SFM, any of which may or may not include TiO_2 particles, as well as separate TiO_2 particles and agglomerates, with biocoronas composed of various food and/or digestive macromolecules. The methods used for these analyses (laser Doppler electrophoresis for ζ-potentials and Multi-angle laser diffraction for size characterization) do not distinguish among these different types of particles.

Particles in undigested SFM, SFM + TiO_2, and FFM + TiO_2 were strongly negatively charged (ζ-potentials = −44.3 ± 1.7, −44.0 ± 0.6, and −40.5 ± 0.5, respectively). Particles in the corresponding small intestinal digestas, as well as in digestas of FFM alone, were also negatively charged, but less strongly than those in undigested suspensions. The ζ-potentials of digestas of FFM, with or without TiO_2, were about half that of undigested FFM with TiO_2 (−20.9 ± 0.2 and −20.9 ± 0.7, respectively), and ζ-potentials of SFM digestas, with or without TiO_2, were roughly three fourths those of the corresponding undigested suspensions (−27.6 ± 0.8 and −32.2 ± 0.9, respectively).

The volume-weighted size distributions of SFM alone, and of SFM and FFM with TiO_2, prior to digestion (Figure 2A) all contained a dominant major peak at about 1 μm, and a smaller peak in the 0.2–0.5 μm range, with a left tail extending into the nano (<100 nm) range. Distributions of SFM, with or without TiO_2, unlike that of FFM with TiO_2, also featured broad peaks of larger agglomerates between 10 and 100 μm in diameter. The mean and cumulative percentile diameters from MALD analysis (Table 1) were consistent with the size distributions. The surface area-weighted mean, D[3,2], also known as the Sauter mean, was smallest in FFM + TiO_2 (0.14 ± 0.01 μm), consistent with the lack of large agglomerates in the size distribution of that suspension, and somewhat larger in SFM and SFM + TiO_2 (0.46 ± 0.01 and 0.52 ± 0.01 μm). The volume-weighted size averages, denoted D[4,3], also known as the DeBroukere means, of these undigested suspensions were considerably larger than the corresponding Sauter means (0.60 ± 0.01, 9.89 ± 0.05, and 9.39 ± 1.81 μm in FFM + TiO_2, SFM + TiO_2, and SFM alone, respectively), as is commonly the case with MALD analysis, but were also much larger in SFM suspensions (with or without TiO_2) than in FFM with TiO_2 (9.39 ± 1.81 in SFM and 9.89 ± 0.05 μm in SFM + TiO_2 vs. 0.60 ± 0.01 μm in FFM + TiO_2). The presence of large agglomerates in the SFM suspensions, and the absence of such agglomerates in the FFM + TiO_2 suspension, were most strongly reflected in the cumulative volume percentile size values (Table 1), denoted Dv10, Dv50, and Dv90, representing the 10^{th}, 50^{th}, and 90^{th} size percentiles of the cumulative particle volume of a sample. Specifically, the smallest 90% of particles in FFM + TiO_2 had sizes equal to or smaller than 1.07 ± 0.01 μm (Dv90), whereas particles in the corresponding 90% of particles in SFM and SFM + TiO_2 suspensions were as large as 29.9 ± 2.3 and 37.5 ± 0.4 μm, respectively.

The size distributions of digestas from SFM and FFM suspensions (Figure 2B) featured single dominant, broad peaks with prominent shoulders or adjoining minor peaks, and in the cases of digestas with TiO_2, small peaks in the millimeter range. The major peaks of TiO_2-containing digestas were substantially left-shifted relative to those of the corresponding food model only suspensions (from ~5 to ~1 μm for FFM, and from ~30 to ~2 μm for SFM suspensions), suggesting that the presence of TiO_2 somehow reduced or prevented

agglomeration of digestive proteins during digestion. However, digestas containing TiO_2 also contained small amounts of very large agglomerates represented by peaks at ~0.6 mm in FFM + TiO_2 and ~1.5 mm in SFM + TiO_2.

As with undigested suspensions, the mean and cumulative percentile diameters of digestas (Table 1) were, for the most part, consistent with their size distributions. The surface area-weighted Sauter means, D[3,2], were several fold larger than those of the undigested suspensions (e.g., 1.46 ± 0.05 vs. 0.14 ± 0.01 μm for FFM + TiO_2, and 2.29 ± 0.07 vs. 0.52 ± 0.01 μm for SFM + TiO_2), and about 3 to 4 fold larger in digestas without TiO_2 than in those with TiO_2 (e.g., 6.73 ± 0.02 μm for SFM alone vs. 2.29 ± 0.07 μm for SFM + TiO_2), consistent with the left shift of major peaks in the distributions of TiO_2-containing digestas noted above. The volume-weighted DeBroukere means, D[4,3], in contrast, were roughly 2 fold smaller in digestas without TiO_2 (e.g., 16.7 ± 1.7 μm for FFM alone vs. 35.8 ± 9.6 μm for FFM + TiO_2). This was somewhat puzzling, given the apparent strong left shift of most of the AUC of the distribution when TiO_2 was present. It is possible that the calculation of D[4,3] gave greater weight to larger particles, such as those in the small peaks at ~0.6 mm in FFM + TiO_2 and at ~1.5 mm in SFM + TiO_2, than their apparent weights in the volume distribution histograms.

In vitro toxicity of food-grade TiO_2 (E171)

In vitro cellular toxicity was evaluated for small intestinal digestas of the food model controls, and of food models containing TiO_2 (E171) at concentrations of 0.75% and 1.5% w/w. Toxicity results are summarized in Figure 3 A, B and C for ENMs in fasting food model (FFM) and in Figure 3 D, E and F for ENMs in standardized food model (SFM).

No differences in TEER values were observed between untreated cells, food model controls, and food models containing TiO_2 (E171) at either concentration tested, indicating that cell layer and tight junction integrity were not affected by any of the treatments. Changes in ROS production after 6 hours of exposure to digestas (relative to cells cultured in fresh medium) are shown in Figure 3 B and E. The positive control (100 μM menadione) induced a 2.4-fold change in ROS production. The difference in ROS production between FFM alone and untreated cells was negligible. In contrast, SFM alone induced a slight but statistically significant increase in ROS production (1.24-fold, $p<0.05$). Similar results were observed in cytotoxicity measured by LDH assay after 24 hours of exposure to digestas. FFM alone caused no increase in cytotoxicity, whereas SFM alone caused a slight although statistically insignificant increase in cytotoxicity (7.5%, $p>0.05$).

At the lower concentration of 0.75% w/w in FFM, TiO_2 had no effect on ROS production, but produced a small, statistically significant increase (7%, $p<0.01$) in cytotoxicity. At 1.5% w/w in FFM, TiO_2 caused a statistically significant increases over FFM control in both ROS production (1.24-fold, $p<0.01$), and cytotoxicity (24%, $p<0.001$). In contrast, TiO_2 in SFM at either dose caused no significant cytotoxicity, and produced only a slight increase in ROS production compared to SFM alone, suggesting that the effect of a more complex food matrix in this case was to eliminate the slight toxicity observed with TiO_2 in FFM..

Proteomic analysis of triculture exposed to TiO_2

The proteomic analysis resulted in the identification of 4944 proteins in total, in which 2271 proteins were quantified across all samples (Supplemental Data 1). Reproducibility analysis among replicates showed a less than 10% coefficient of variation (CV) for most proteins (Figure S1), demonstrating the robustness of the workflow. In order to visualize the overall quantitative patterns across all samples, an unsupervised clustering was used to analyze the proteomic data (Figure. S2). The result revealed two distinct sample groups corresponding to the two food models used in the study. Within each food matrix cluster, similar overall patterns of protein abundances were observed between the food model control (FFM alone and SFM alone) and TiO_2-treated samples, suggesting that TiO_2 within each food matrix induced a minimum impact on the cellular proteomes.

Impact of TiO_2 and food matrix on the cellular proteome

The two-factor experimental design made it possible to perform multiple comparisons to determine the effect of ENM treatment (TiO_2 vs control) and food matrix (control or TiO_2 treatment with two different food matrices). Statistical analyses of the proteomes were represented as volcano (scatter) plots, in which the change in protein abundance (log2 fold change) and the statistical significance (-log adjusted p value) of each protein is depicted as a point (Figure 4 and Figure 5). No significantly altered proteins were identified in cells treated with digestas from FFM containing TiO_2 at either concentration (Figure 4A and B). A similar result was observed in digestas from TiO_2 in SFM, with only 28 significant proteins found at the low dose of TiO_2 treatment (Figure 4C, Supplemental Data 2), and no significant proteins detected at the high dose of TiO_2 (Figure 4D). Visualization of the proteome analyses shows that the log2 fold change was narrowly distributed (majority of proteins falling between −0.5 and 0.5), with only a few proteins showing more than a 2-fold change (log2 fold change > 1, Figure 4).

The impact of food matrix on cellular proteomes was evaluated by comparing samples with the same TiO_2 concentration (0% (control), 0.75% or 1.5%) but with different food matrices. In these comparisons, hundreds of proteins were identified as statistically significant with abundance differences (Figure 5, Supplemental Data 2). Significant differences were observed between the two food model controls (245 proteins). The number of differentially expressed proteins between FFM containing high dose of TiO_2 and SFM containing high dose of TiO_2 was somewhat greater (530 proteins) (Figure 5 A vs. 5 C). At the low TiO_2 dose, the number of differentially expressed proteins between FFM and SFM was considerably lower (85 proteins). Together, these data show that the food matrix significantly affects the proteome of the triculture system, whereas TiO_2 itself has relatively little impact, but may amplify or modulate the differences caused by the food model.

Food matrix-associated differential proteins and cellular processes

To identify cellular pathways and biological processes affected by the food matrix, differentially expressed proteins between the two food matrixes (alone and with TiO_2 at each dose) were subjected to gene ontology (GO) based enrichment analysis. Cellular processes identified, and the significance of their enrichment (represented as $-\log_{10}$ p value), in each of the three comparisons were shown in Figure 6A, in which the significance of the

enrichment was indicated by the negative log p value. Several biological processes, including cell-cell adhesion, translation, and tricarboxylic acid cycle (TCA) were significantly enriched in all comparisons of the two food matrixes, suggesting a consistent food matrix effect on the cellular proteome, regardless of the presence of TiO_2. Most biological processes were less significantly enriched by food model in the presence of TiO_2 at lower dose, consistent with the relatively small number of significant proteins observed in this comparison.

In order to visualize food matrix-associated protein abundance changes in these biological processes, we compared the relative protein abundance between FFM and SFM for selected proteins (Figure 6 B). Higher abundances of all selected proteins were observed in the triculture system after treatment with digesta from SFM, relative to treatment with FFM (regardless of presence or concentration of TiO_2). A prominent example of a biological processes up-regulated by SFM was the TCA cycle, where core enzymes (SUCA, MDHC, SDHA, ACON, and IDHC) had significantly higher abundances in cells treated with SFM digestas than those treated with FFM digestas. Likewise, SFM caused upregulation in proteins involved in gluconeogenesis and protein synthesis (translation), as well as in mitochondrial proteins involved in oxidation-reduction processes, including MMSA (methylmalonate-semialdehyde dehydrogenase, mitochondrial) and DHE3 (glutamate dehydrogenase 1, mitochondrial). The upregulation of metabolic activities and oxidation-reduction processes by SFM relative to FFM suggests a higher level of energy metabolism and redox control after ingestion of a standardized complete diet relative to a fasting diet.

Discussion

The increasing use of engineered nanomaterials, such as TiO_2, in food raises concerns about potential health risks from various stakeholders [26]. To accelerate the science based implementation of related regulations, a comprehensive understanding of the toxicity of ingested ENMs is required.

In this study, we assessed the cytotoxicity and proteomic effects of food-grade TiO_2 (E171), which contains a considerable portion of nano-scale particles (approximately 40% by number). In order to bring physiological relevance to this *in vitro* cellular study, two different food models (FFM and SFM) were evaluated, and a gastrointestinal tract (GIT) simulator was used to mimic oral, gastric, and small intestinal digestion. This integrated approach take into consideration interactions of TiO_2 with food matrix and potential property transformations across the GIT which are known modulators of bioactivity [13,14,21,33]. The final small intestinal phase digesta was applied to a tri-culture small intestinal epithelium model to assess the cytotoxicity and impact on the cellular proteome of food-grade TiO_2 (E171) rather than using the ENM mixed with culture medium alone which is usually the practice in nanotoxicology research of ingested ENMs.

At starting concentrations of 0.75% and 1.5% w/w in FFM or SFM (final concentrations in the digesta-cell culture medium mixture of 150 μg/mL and 300 μg/mL), TiO_2 (E171) caused little or no cytotoxicity in the tri-culture small intestinal epithelium model. This contrasts somewhat with numerous reports of cell culture studies, which found that industrial grade

but not a food-grade, uniform 20 nm TiO_2 (P25), used for paintings, printing inks, and plastics, as well as other very small (5–10 nm) TiO_2 nanoparticles, cause considerable cytotoxicity in concentrations ranging from 50 μg/mL to 2 mg/mL in cell culture medium [44–46]. The cytotoxicity was presumably from the extremely small size of TiO_2 used in these studies. However, in the case of food-grade TiO_2 (E171) with an average size around 110 nm, the low cytotoxicity reported here is consistent with previous reports. Chen et al. extracted TiO_2 particles from chewing gum to evaluate their cytotoxicity in gastrointestinal cells, and found that gum nano-TiO_2 particles caused little cytotoxicity after a 24 h exposure at 200 μg/mL in cell culture medium [25]. Similarly, in Dorier et al.'s study with co-culture intestinal epithelial cells, in which cells were either continuously or repeatedly exposed to TiO_2 (E171) at 100 μg/mL in cell culture medium [47], no differences were observed in viability, tight junction or microvilli morphology, or mucus secretion, between treatment and control cells. However, a slight increase in intracellular ROS was detected (similar to the slight increase in ROS reported here for digested E171 in FFM, but not in SFM), and continuous exposure was found to induced significant oxidative damage to DNA. The aforementioned studies provide valuable information about the interaction between an *in vitro* model of small intestinal epithelium and pristine food-grade TiO_2 in cell culture medium, but do not account for the effects of interactions of the TiO_2 with the food matrix and GIT fluids and conditions during digestion, which may modify the oral toxicity of ingested ENMs.

Interestingly, SFM eliminated the slight toxicity of TiO_2 (E171) observed in FFM. It is well known that adsorption of proteins, lipids, and other molecules from the surroundings alter the surface characteristics of ENMs [11,23,27,48]. The formation of a biological corona impacts the cellular and tissue responses to ENMs [49–51]. For example, the binding of blood proteins to carbon nanotubes (CNTs) reduced their cytotoxic effect on human umbilical vein endothelial cells and acute monocytic leukemia cells by protecting them from direct contact with the bare surfaces of CNTs [52]. In the present study, TiO_2 nanoparticles may have adsorbed some of the constituents in SFM, thereby masking harmful surface atoms and groups, and otherwise altering surface characteristics and possibly cellular uptake resulting in reduced cytotoxicity. Moreover, the observed differences between the use of the two food models can also be a result of differential agglomeration and settling of formed agglomerates which contribute to differences in doses delivered to the cells. However, the delivered dose in digesta cannot be measured using our previous dosimetry model which was developed for nanoparticles administrated to cells in cell culture medium [53–55]. The complexity of digestas make measurement of effective density of ingested ENMs impossible [56]. More mechanistic studies are needed to understand the role of biological coronas and delivered dose in reducing the bioactivity in the presence of SFM model.

MS-based quantitative proteomics has become a robust tool that provides identification and quantification of thousands of proteins in biological samples. It has been increasingly used to study the biological impact of exposure to ENMs in biological systems, including TiO_2 [34–41]. These studies have shown that ENMs can alter many cellular processes, including metabolism, protein translation, response to ROS, cytoskeleton remodeling, and immune responses. Despite the wealth of information about potential biological effect of ENMs provided by these proteomic studies, the oral route of exposure and impact of the food

matrix on the ability of ENMs to trigger cellular responses has not been evaluated to the best of our knowledge. In addition, many of these investigations employed laborious and time-consuming gel-based proteomic approaches [41,42], in which low proteome coverage and poor quantitative reproducibility are limiting.

The proteomic approach employed in this study provides an unbiased quantitative analysis of the impact of TiO_2, as well as that of the food matrix, at the proteome-wide level. The similarity of the proteomes of TiO_2-treated and untreated samples, regardless of food model, validated our observation that food-grade TiO_2 in either food models causes little or no cytotoxicity. However, results from previous *in vitro* and *in vivo* studies of the impact of TiO_2 on the proteome are inconsistent [34–36,38]. For example, Chen *et al.* found that the abundance of nearly 1000 proteins in mouse bone marrow derived macrophages were significantly changed after 24 h treatment with 100 μg/mL TiO_2 nanoparticles (10 nm, anatase) in cell culture media [57]. In contrast, Triboulet *et al.* employed the same dose (100 μg/mL) of TiO_2 nanoparticles (25 nm, anatase) in mouse macrophages and observed relatively few changes in the proteome, as exemplified by the identification of only seven proteins whose abundance was significantly changed (>20%) by exposure to TiO_2 nanoparticles (in cell culture media) [41]. This discrepancy is likely due to differences in particle sizes, cell lines, and experimental schemes (i.e. different sizes and composition TiO_2 nanoparticles were used and their dissolution kinetics and transformations across the GIT were ignored [27]).

It is notable that in the present study, food-grade TiO_2 (E171) with an average size of 110 nm was first dispersed in a food model, and the resulting mixture was then subjected to physiological digestion, before applied to cells. This approach recapitulates the interactions of TiO_2 with food and digestive tract secretions that would normally occur during digestion, and prior to contact with the small intestinal epithelium. These interactions could alter surface charges or oxidation states, or result in adsorption of food and digestive molecules, which could neutralize or mask reactive surface groups, and otherwise render the TiO_2 particles less toxic. Moreover, the tri-culture model used in this study represents a realistic hybrid model of the complete small intestinal epithelium.

Although the direct impact of TiO_2 on the proteome was negligible, more significant and substantial differences in protein abundance profiles were found between the FFM- and SFM-treated cells. The consistent expression patterns within each category of samples (FFM and SFM) and the differential regulation between the two categories clearly separated the FFM-proteomes and the SFM-proteomes. This confirms that the effect of TiO_2 itself on the proteome is minimal in both food models and reveals a more dominant effect of the food matrix on the small intestinal epithelial cellular proteome. Compared to FFM, SFM induced proteome changes suggesting increases in cellular activities involved in energy metabolism (TCA cycle, gluconeogenesis) and protein biosynthesis (translation). The TCA cycle is the metabolism hub, producing ATP, NADH and other metabolite intermediates through the oxidation of acetyl-CoA. Food availability would likely trigger the catabolism of carbohydrates, fats, and proteins, generating acetyl-CoA as the common substrate for the TCA cycle. The increased availability of acetyl-CoA might, through as yet unknown mechanisms, increase synthesis of TCA cycle enzymes. Indeed, multiple enzymes in the

TCA cycle were up-regulated in SFM samples. Such increased metabolic activity in mitochondria is also consistent with the increased expression of many metabolic enzymes involving in the oxidation-reduction process since many of these enzyme activities are redox-dependent [58]. Increased mitochondrial energy metabolism in SFM digesta treated cells could also lead to higher levels of ROS generation, as mitochondria are one of the major sources of ROS production in mammalian cells [59,60]. This is consistent with the finding of slightly higher levels of with SFM than with FFM digesta treatments (Figure 3 E). Moderate levels of ROS can activate the antioxidant defense system, which is reflected in the up-regulation of the peroxidase GPX4 observed in SFM digesta-treated cells. It is notable that other proteins involved in the oxidation-reduction process, such as HIG1A, showed higher abundance in FFM than in SFM digesta-treated cells. HIG1A is a mitochondrial inner membrane protein that has been shown to play a protective role against oxidative stress by promoting mitochondrial homeostasis [61]. Thus, it is possible that higher ROS generation in the SFM digesta treated cells was quenched by the antioxidant system, not necessarily leading to oxidative stress. Instead, the nutrient-poor FMM could trigger slight cellular stress, which further activate an increase of HIG1A. Interestingly, SFM treatments also caused an up-regulation of cell-cell adhesion molecules, including two septins (SEPT7 and SEPT9), plasma membrane-associated cytoskeletal components required for cadherin-mediated cellular junctions [62–64]. Given that cell-cell adhesion molecules, such as cadherins and integrins, participate in intercellular adhesion of Caco2/HT-29 [65,66], we speculate that this up-regulation of cell-cell adhesion proteins may promote the maintenance and integrity of these critical intercellular junctions.

In addition, a greater number of significantly different proteins were observed between the SFM- and FFM-treated cells in the presence of high dose of TiO_2 than without TiO_2 (Figure 5), suggesting that the interaction of TiO_2 and food models may affect the proteome. The actual cause of this effect is currently unknown and requires further studies. The effects of TiO_2 on digestion and absorption of some food components have been reported. For example, TiO_2 can decrease the bioaccessibility and bioavailability of several nutrients, including iron, zinc, fatty acids [67], and dietary flavonoids [68]. TiO_2 can also disrupt the structure of the dietary protein, casein, resulting in a decrease in its hydrolysis in the stomach [69]. On the other hand, TiO_2 can increase the toxicity and bioavailability of pesticide residues in foods [28]. All these findings highlight the importance of considering the food matrix when studying the implications of ingested ENMs, not only because the food matrix may alter the cytotoxicity of the ENMs, but also because the ENMs may affect the cellular responses to the food matrix. Nevertheless, since no *in vitro* model can perfectly mimic the mechanical, biochemical, and biological conditions or cellular responses in the human gastrointestinal tract, future animal studies are required for a comprehensive assessment of the oral toxicity of the food additive TiO_2 (E171).

Conclusion

In this study, the cytotoxicity, and effects on the cellular proteome, of the food additive TiO_2 (E171) in a tri-culture small intestinal epithelium, were investigated. Food matrix effects on bioactivity were also assessed using a fasting food model (FFM), and a standardized food model (SFM) which is based on the average American diet. The results of these studies

demonstrated that the food additive TiO_2 (E171) is relatively non cytotoxic for the small intestinal epithelium under the experimental conditions tested. However, significant and substantial differences in protein abundance profiles were observed between the FFM digesta- and SFM digesta-treated cells, and a greater number of significantly different proteins were observed between the SFM digesta- and FFM digesta-treated cells in the presence of high dose of TiO_2 than without TiO_2. Additional studies, and corresponding *in vivo* studies, focused on the interactions of ingested TiO_2 ENMs with the food matrix and digestive processes and cells are necessary. Understanding the full implications of the increasing amounts of ENMs entering the food stream will provide regulators with useful data and facilitate development of safer-by-design food-grade ingested nanomaterials.

Supplementary Material

Refer to Web version on PubMed Central for supplementary material.

Acknowledgements

The engineered nanomaterials used in the research presented in this publication were characterized and provided by the Engineered Nanomaterials Resource and Coordination Core established at Harvard T. H. Chan School of Public Health (NIH grant # U24ES026946) as part of the Nanotechnology Health Implications Research (NHIR) Consortium. The content is solely the responsibility of the authors and does not necessarily represent the official view of the National Institutes of Health. Portions of the work were supported by the National Institutes of Health Grants U01ES027292 and U24ES026946. The proteomic experimental work described herein was performed in the Environmental Molecular Sciences Laboratory, Pacific Northwest National Laboratory, a national scientific user facility sponsored by the Department of Energy under Contract DE-AC05-76RL0 1830.

References

1. DeLoid GM, Sohal IS, Lorente LR, Molina RM, Pyrgiotakis G, Stevanovic A, Zhang R, McClements DJ, Geitner NK, Bousfield DW, Ng KW, Loo SCJ, Bell DC, Brain J and Demokritou P, Reducing Intestinal Digestion and Absorption of Fat Using a Nature-Derived Biopolymer: Interference of Triglyceride Hydrolysis by Nanocellulose, ACS Nano, 2018, 12, 6469–6479. [PubMed: 29874029]
2. Vaze N, Pyrgiotakis G, Mena L, Baumann R, Demokritou A, Ericsson M, Zhang Y, Bello D, Eleftheriadou M and Demokritou P, A nano-carrier platform for the targeted delivery of nature-inspired antimicrobials using Engineered Water Nanostructures for food safety applications, Food Control, 2019, 96, 365–374.
3. Eleftheriadou M, Pyrgiotakis G and Demokritou P, Nanotechnology to the rescue: using nano-enabled approaches in microbiological food safety and quality, Curr. Opin. Biotechnol, 2017, 44, 87–93. [PubMed: 27992831]
4. Schoepf JJ, Bi Y, Kidd J, Herckes P, Hristovski K and Westerhoff P, Detection and dissolution of needle-like hydroxyapatite nanomaterials in infant formula, NanoImpact, 2017, 5, 22–28.
5. Chen H, Seiber JN and Hotze M, ACS select on nanotechnology in food and agriculture: A perspective on implications and applications, J. Agric. Food Chem, 2014, 62, 1209–1212. [PubMed: 24479582]
6. Rhodes CJ, Current Commentary Eating small : applications and implications for nano- technology in agriculture and the food industry, Sci. Prog, 2014, 97, 173–182. [PubMed: 25110799]
7. Pyrgiotakis G, Luu W, Zhang Z, Vaze N, DeLoid G, Rubio L, Graham WAC, Bell DC, Bousfield D and Demokritou P, Development of high throughput, high precision synthesis platforms and characterization methodologies for toxicological studies of nanocellulose, Cellulose, 2018, 25, 2303–2319. [PubMed: 31839698]

8. Sampathkumar K, Riyajan S, Tan CK, Demokritou P, Chudapongse N and Loo SCJ, Small-Intestine-Specific Delivery of Antidiabetic Extracts from Withania coagulans Using Polysaccharide-Based Enteric-Coated Nanoparticles, ACS Omega, 2019, 4, 12049–12057. [PubMed: 31460318]
9. Servin AD and White JC, Nanotechnology in agriculture: Next steps for understanding engineered nanoparticle exposure and risk, NanoImpact, 2016, 1, 9–12.
10. Schoepf JJ, Bi Y, Kidd J, Herckes P, Hristovski K and Westerhoff P, Detection and dissolution of needle-like hydroxyapatite nanomaterials in infant formula, NanoImpact, 2017, 5, 22–28.
11. Sohal IS, O'Fallon KS, Gaines P, Demokritou P and Bello D, Ingested engineered nanomaterials: state of science in nanotoxicity testing and future research needs, Part. Fibre Toxicol, 2018, 15, 29. [PubMed: 29970114]
12. Sohal IS, Cho YK, O'Fallon KS, Gaines P, Demokritou P and Bello D, Dissolution Behavior and Biodurability of Ingested Engineered Nanomaterials in the Gastrointestinal Environment, ACS Nano, 2018, 12, 8115–8128. [PubMed: 30021067]
13. McClements DJ, DeLoid G, Pyrgiotakis G, Shatkin JA, Xiao H and Demokritou P, NanoImpact, 2016, 3–4, 47–57.
14. Sohal IS, O'Fallon KS, Gaines P, Demokritou P and Bello D, Ingested engineered nanomaterials: state of science in nanotoxicity testing and future research needs, Part. Fibre Toxicol, 2018, 15, 29. [PubMed: 29970114]
15. Wang Y, Chen Z, Ba T, Pu J, Chen T, Song Y, Gu Y, Qian Q, Xu Y, Xiang K, Wang H and Jia G, Susceptibility of Young and Adult Rats to the Oral Toxicity of Titanium Dioxide Nanoparticles, Small, 2013, 9, 1742–1752. [PubMed: 22945798]
16. Lu X, Miousse IR, Pirela SV, Moore JK, Melnyk S, Koturbash I and Demokritou P, In vivo epigenetic effects induced by engineered nanomaterials: A case study of copper oxide and laser printer-emitted engineered nanoparticles, Nanotoxicology, 2016, 10, 629–639. [PubMed: 26559097]
17. Pirela SV, Bhattacharya K, Wang Y, Zhang Y, Wang G, Christophi CA, Godleski J, Thomas T, Qian Y, Orandle MS, Sisler JD, Bello D, Castranova V and Demokritou P, A 21-day sub-acute, whole-body inhalation exposure to printer-emitted engineered nanoparticles in rats: Exploring pulmonary and systemic effects, NanoImpact, 2019, 15, 100176.
18. DeLoid G, Casella B, Pirela S, Filoramo R, Pyrgiotakis G, Demokritou P and Kobzik L, Effects of engineered nanomaterial exposure on macrophage innate immune function, NanoImpact, 2016, 2, 70–81. [PubMed: 29568809]
19. Konduru NV, Murdaugh KM, Swami A, Jimenez RJ, Donaghey TC, Demokritou P, Brain JD and Molina RM, Surface modification of zinc oxide nanoparticles with amorphous silica alters their fate in the circulation, Nanotoxicology, 2016, 10, 720–727. [PubMed: 26581431]
20. Lu X, Miousse IR, Pirela SV, Melnyk S, Koturbash I and Demokritou P, Short-term exposure to engineered nanomaterials affects cellular epigenome, Nanotoxicology, 2016, 10, 140–150. [PubMed: 25938281]
21. DeLoid GM, Wang Y, Kapronezai K, Lorente LR, Zhang R, Pyrgiotakis G, Konduru NV, Ericsson M, White JC, De La Torre-Roche R, Xiao H, McClements DJ and Demokritou P, An integrated methodology for assessing the impact of food matrix and gastrointestinal effects on the biokinetics and cellular toxicity of ingested engineered nanomaterials, Part. Fibre Toxicol, 2017, 14, 40. [PubMed: 29029643]
22. McClements DJ, DeLoid G, Pyrgiotakis G, Shatkin JA, Xiao H and Demokritou P, The role of the food matrix and gastrointestinal tract in the assessment of biological properties of ingested engineered nanomaterials (iENMs): State of the science and knowledge gaps, NanoImpact, 2016, 3–4, 47–57.
23. McClements DJ and Xiao H, Is nano safe in foods? Establishing the factors impacting the gastrointestinal fate and toxicity of organic and inorganic food-grade nanoparticles, npj Sci. Food, 2017, 1, 6. [PubMed: 31304248]
24. Sohal IS, O'Fallon KS, Gaines P, Demokritou P and Bello D, Ingested engineered nanomaterials: State of science in nanotoxicity testing and future research needs, Part. Fibre Toxicol,, DOI:10.1186/s12989-018-0265-1.

25. Chen X-X, Cheng B, Yang Y-X, Cao A, Liu J-H, Du L-J, Liu Y, Zhao Y and Wang H, Characterization and Preliminary Toxicity Assay of Nano-Titanium Dioxide Additive in Sugar-Coated Chewing Gum, Small, 2013, 9, 1765–1774. [PubMed: 23065899]
26. Weir A, Westerhoff P, Fabricius L, Hristovski K and von Goetz N, Titanium Dioxide Nanoparticles in Food and Personal Care Products, Environ. Sci. Technol, 2012, 46, 2242–2250. [PubMed: 22260395]
27. Lee JY, Wang H, Pyrgiotakis G, DeLoid GM, Zhang Z, Beltran-Huarac J, Demokritou P and Zhong W, Analysis of lipid adsorption on nanoparticles by nanoflow liquid chromatography-tandem mass spectrometry, Anal. Bioanal. Chem, 2018, 410, 6155–6164. [PubMed: 29845324]
28. Cao X, DeLoid G, Bitounis D, De La Torre R, White J, Zhang Z, Ho CG, Ng KW, Eitzer B and Demokritou P, Co-exposure to the food additives SiO2 (E551) or TiO2 (E171) and the pesticide boscalid increases cytotoxicity and bioavailability of the pesticide in a tri-culture small intestinal epithelium model: Potential health implications, Environ. Sci. Nano,, DOI:10.1039/C9EN00676A.
29. Setyawati MI, Sevencan C, Bay BH, Xie J, Zhang Y, Demokritou P and Leong DT, Nano-TiO2 Drives Epithelial–Mesenchymal Transition in Intestinal Epithelial Cancer Cells, Small,, DOI:10.1002/smll.201800922.
30. Wang J, Zhou G, Chen C, Yu H, Wang T, Ma Y, Jia G, Gao Y, Li B, Sun J, Li Y, Jiao F, Zhao Y and Chai Z, Acute toxicity and biodistribution of different sized titanium dioxide particles in mice after oral administration, Toxicol. Lett, 2007, 168, 176–185. [PubMed: 17197136]
31. Cho W-S, Kang B-C, Lee JK, Jeong J, Che J-H and Seok SH, Comparative absorption, distribution, and excretion of titanium dioxide and zinc oxide nanoparticles after repeated oral administration, Part. Fibre Toxicol, 2013, 10, 9. [PubMed: 23531334]
32. Jain A, Ranjan S, Dasgupta N and Ramalingam C, Nanomaterials in food and agriculture: An overview on their safety concerns and regulatory issues, Crit. Rev. Food Sci. Nutr, 2018, 58, 297–317. [PubMed: 27052385]
33. Zhang Z, Zhang R, Xiao H, Bhattacharya K, Bitounis D, Demokritou P and McClements DJ, Development of a standardized food model for studying the impact of food matrix effects on the gastrointestinal fate and toxicity of ingested nanomaterials, NanoImpact, 2019, 13, 13–25. [PubMed: 31093583]
34. Jeon Y-M, Park S-K and Lee M-Y, Toxicoproteomic identification of TiO 2 nanoparticle-induced protein expression changes in mouse brain, Animal Cells Syst. (Seoul), 2011, 15, 107–114.
35. Jeon Y-M, Park S-K, Rhee S-K and Lee M-Y, Proteomic profiling of the differentially expressed proteins by TiO2 nanoparticles in mouse kidney, Mol. Cell. Toxicol, 2010, 6, 414–420.
36. Sund J, Palomäki J, Ahonen N, Savolainen K, Alenius H and Puustinen A, Phagocytosis of nano-sized titanium dioxide triggers changes in protein acetylation, J. Proteomics, 2014, 108, 469–483. [PubMed: 24972317]
37. Armand L, Biola-Clier M, Bobyk L, Collin-Faure V, Diemer H, Strub J-M, Cianferani S, Van Dorsselaer A, Herlin-Boime N, Rabilloud T and Carriere M, Molecular responses of alveolar epithelial A549 cells to chronic exposure to titanium dioxide nanoparticles: A proteomic view, J. Proteomics, 2016, 134, 163–173. [PubMed: 26276045]
38. Maurer MM, Donohoe GC, Maleki H, Yi J, McBride C, Nurkiewicz TR and Valentine SJ, Comparative plasma proteomic studies of pulmonary TiO2 nanoparticle exposure in rats using liquid chromatography tandem mass spectrometry, J. Proteomics, 2016, 130, 85–93. [PubMed: 26375203]
39. Nath Roy D, Goswami R and Pal A, Nanomaterial and toxicity: what can proteomics tell us about the nanotoxicology?, Xenobiotica, 2017, 47, 632–643. [PubMed: 27414072]
40. Zhang T, Gaffrey MJ, Thrall BD and Qian W-J, Mass spectrometry-based proteomics for system-level characterization of biological responses to engineered nanomaterials, Anal. Bioanal. Chem, 2018, 410, 6067–6077. [PubMed: 29947897]
41. Triboulet S, Aude-Garcia C, Armand L, Collin-Faure V, Chevallet M, Diemer H, Gerdil A, Proamer F, Strub J-M, Habert A, Herlin N, Van Dorsselaer A, Carrière M and Rabilloud T, Comparative Proteomic Analysis of the Molecular Responses of Mouse Macrophages to Titanium Dioxide and Copper Oxide Nanoparticles Unravels Some Toxic Mechanisms for Copper Oxide Nanoparticles in Macrophages, PLoS One, 2015, 10, e0124496. [PubMed: 25902355]

42. Georgantzopoulou A, Serchi T, Cambier S, Leclercq CC, Renaut J, Shao J, Kruszewski M, Lentzen E, Grysan P, Eswara S, Audinot J-N, Contal S, Ziebel J, Guignard C, Hoffmann L, Murk AJ and Gutleb AC, Effects of silver nanoparticles and ions on a co-culture model for the gastrointestinal epithelium, Part. Fibre Toxicol, 2015, 13, 9.
43. Mahler GJ, Esch MB, Tako E, Southard TL, Archer SD, Glahn RP and Shuler ML, Oral exposure to polystyrene nanoparticles affects iron absorption, Nat. Nanotechnol, 2012, 7, 264–271. [PubMed: 22327877]
44. Gerloff K, Fenoglio I, Carella E, Kolling J, Albrecht C, Boots AW, Förster I and Schins RPF, Distinctive Toxicity of TiO $_2$ Rutile/Anatase Mixed Phase Nanoparticles on Caco-2 Cells, Chem. Res. Toxicol, 2012, 25, 646–655. [PubMed: 22263745]
45. Krüger K, Cossais F, Neve H and Klempt M, Titanium dioxide nanoparticles activate IL8-related inflammatory pathways in human colonic epithelial Caco-2 cells, J. Nanoparticle Res, 2014, 16, 2402.
46. Dorier M, Brun E, Veronesi G, Barreau F, Pernet-Gallay K, Desvergne C, Rabilloud T, Carapito C, Herlin-Boime N and Carrière M, Impact of anatase and rutile titanium dioxide nanoparticles on uptake carriers and efflux pumps in Caco-2 gut epithelial cells, Nanoscale, 2015, 7, 7352–7360. [PubMed: 25825056]
47. Dorier M, Béal D, Marie-Desvergne C, Dubosson M, Barreau F, Houdeau E, Herlin-Boime N and Carriere M, Continuous *in vitro* exposure of intestinal epithelial cells to E171 food additive causes oxidative stress, inducing oxidation of DNA bases but no endoplasmic reticulum stress, Nanotoxicology, 2017, 1–11.
48. Monopoli MP, Åberg C, Salvati A and Dawson KA, Biomolecular coronas provide the biological identity of nanosized materials, Nat. Nanotechnol, 2012, 7, 779–786. [PubMed: 23212421]
49. Konduru NV, Molina RM, Swami A, Damiani F, Pyrgiotakis G, Lin P, Andreozzi P, Donaghey TC, Demokritou P, Krol S, Kreyling W and Brain JD, Protein corona: implications for nanoparticle interactions with pulmonary cells, Part. Fibre Toxicol, 2017, 14, 42. [PubMed: 29084556]
50. Giri K, Shameer K, Zimmermann MT, Saha S, Chakraborty PK, Sharma A, Arvizo RR, Madden BJ, Mccormick DJ, Kocher J-PA, Bhattacharya R and Mukherjee P, Understanding protein-nanoparticle interaction: a new gateway to disease therapeutics., Bioconjug. Chem, 2014, 25, 1078–90. [PubMed: 24831101]
51. Mahmoudi M, Lynch I, Ejtehadi MR, Monopoli MP, Bombelli FB and Laurent S, Protein −Nanoparticle Interactions: Opportunities and Challenges, Chem. Rev, 2011, 111, 5610–5637. [PubMed: 21688848]
52. Ge C, Du J, Zhao L, Wang L, Liu Y, Li D, Yang Y, Zhou R, Zhao Y, Chai Z and Chen C, Binding of blood proteins to carbon nanotubes reduces cytotoxicity., Proc. Natl. Acad. Sci. U. S. A, 2011, 108, 16968–73. [PubMed: 21969544]
53. Cohen JM, Beltran-Huarac J, Pyrgiotakis G and Demokritou P, Effective delivery of sonication energy to fast settling and agglomerating nanomaterial suspensions for cellular studies: Implications for stability, particle kinetics, dosimetry and toxicity, NanoImpact, 2018, 10, 81–86. [PubMed: 29479575]
54. Cohen J, DeLoid G, Pyrgiotakis G and Demokritou P, Interactions of engineered nanomaterials in physiological media and implications for in vitro dosimetry, Nanotoxicology, 2013, 7, 417–431. [PubMed: 22393878]
55. DeLoid GM, Cohen JM, Pyrgiotakis G and Demokritou P, Preparation, characterization, and in vitro dosimetry of dispersed, engineered nanomaterials, Nat. Protoc, 2017, 12, 355–371. [PubMed: 28102836]
56. Deloid G, Cohen JM, Darrah T, Derk R, Rojanasakul L, Pyrgiotakis G, Wohlleben W and Demokritou P, Estimating the effective density of engineered nanomaterials for in vitro dosimetry, Nat. Commun,, DOI:10.1038/ncomms4514.
57. Chen Q, Wang N, Zhu M, Lu J, Zhong H, Xue X, Guo S, Li M, Wei X, Tao Y and Yin H, TiO2 nanoparticles cause mitochondrial dysfunction, activate inflammatory responses, and attenuate phagocytosis in macrophages: A proteomic and metabolomic insight, Redox Biol, 2018, 15, 266–276. [PubMed: 29294438]
58. Yin F, Boveris A and Cadenas E, Antioxidants Redox Signal., 2014, 20, 353–371.

59. Zorov DB, Juhaszova M and Sollott SJ, Mitochondrial Reactive Oxygen Species (ROS) and ROS-Induced ROS Release, Physiol. Rev, 2014, 94, 909–950. [PubMed: 24987008]
60. Murphy MP, How mitochondria produce reactive oxygen species, Biochem. J, 2009, 417, 1–13. [PubMed: 19061483]
61. Li T, Xian WJ, Gao Y, Jiang S, Yu QH, Zheng QC and Zhang Y, Higd1a Protects Cells from Lipotoxicity under High-Fat Exposure, Oxid. Med. Cell. Longev, 2019, 2019, 6051262. [PubMed: 31089410]
62. Kim J and Cooper JA, Septins regulate junctional integrity of endothelial monolayers, Mol. Biol. Cell, 2018, 29, 1693–1703. [PubMed: 29771630]
63. Füchtbauer A, Lassen LB, Jensen AB, Howard J, de A Quiroga S, Warming S, Sørensen AB, Pedersen FS and Füchtbauer E-M, Septin9 is involved in septin filament formation and cellular stability, Biol. Chem, 2011, 392, 769–777. [PubMed: 21824004]
64. Phan QT, Eng DK, Mostowy S, Park H, Cossart P and Filler SG, Role of endothelial cell septin 7 in the endocytosis of Candida albicans., MBio, 2013, 4, e00542–13. [PubMed: 24345743]
65. Ferraretto A, Bottani M, De Luca P, Cornaghi L, Arnaboldi F, Maggioni M, Fiorilli A and Donetti E, Morphofunctional properties of a differentiated Caco2/HT-29 co-culture as an *in vitro* model of human intestinal epithelium, Biosci. Rep, 2018, 38, BSR20171497. [PubMed: 29540534]
66. Schreider C, Peignon G, Thenet S, Chambaz J and Pinçon-Raymond M, Integrin-mediated functional polarization of Caco-2 cells through E-cadherin--actin complexes., J. Cell Sci, 2002, 115, 543–52. [PubMed: 11861761]
67. Guo Z, Martucci NJ, Moreno-Olivas F, Tako E and Mahler GJ, Titanium dioxide nanoparticle ingestion alters nutrient absorption in an in vitro model of the small intestine, NanoImpact, 2017, 5, 70–82. [PubMed: 28944308]
68. Cao X, Ma C, Gao Z, Zheng J, He L, McClements DJ and Xiao H, Characterization of the Interactions between Titanium Dioxide Nanoparticles and Polymethoxyflavones Using Surface-Enhanced Raman Spectroscopy, J. Agric. Food Chem, 2016, 64, 9436–9441. [PubMed: 27960290]
69. Cao X, Han Y, Li F, Li Z, McClements DJ, He L, Decker EA, Xing B and Xiao H, Impact of protein-nanoparticle interactions on gastrointestinal fate of ingested nanoparticles: Not just simple protein corona effects, NanoImpact, 2019, 13, 37–43.

Highlights

- Food additive TiO_2 (E171) in fasting food model (FFM), but not in standardized food model (SFM), produced significant, dose-dependent cytotoxicity, and at the higher dose caused significant oxidative stress, indicative of a food matrix effect.
- No significant perturbations of the cellular proteome were observed with TiO_2 in either FFM or SFM food models.
- Proteins involved in the tricarboxylic acid (TCA) cycle, gluconeogenesis, and translation were up-regulated by digestas from SFM compared to those from FFM, also indicative of food matrix effects in the case of food models alone.
- The differences in profiles between the two food models was more pronounced in the presence of TiO_2 indicative of food matrix effects

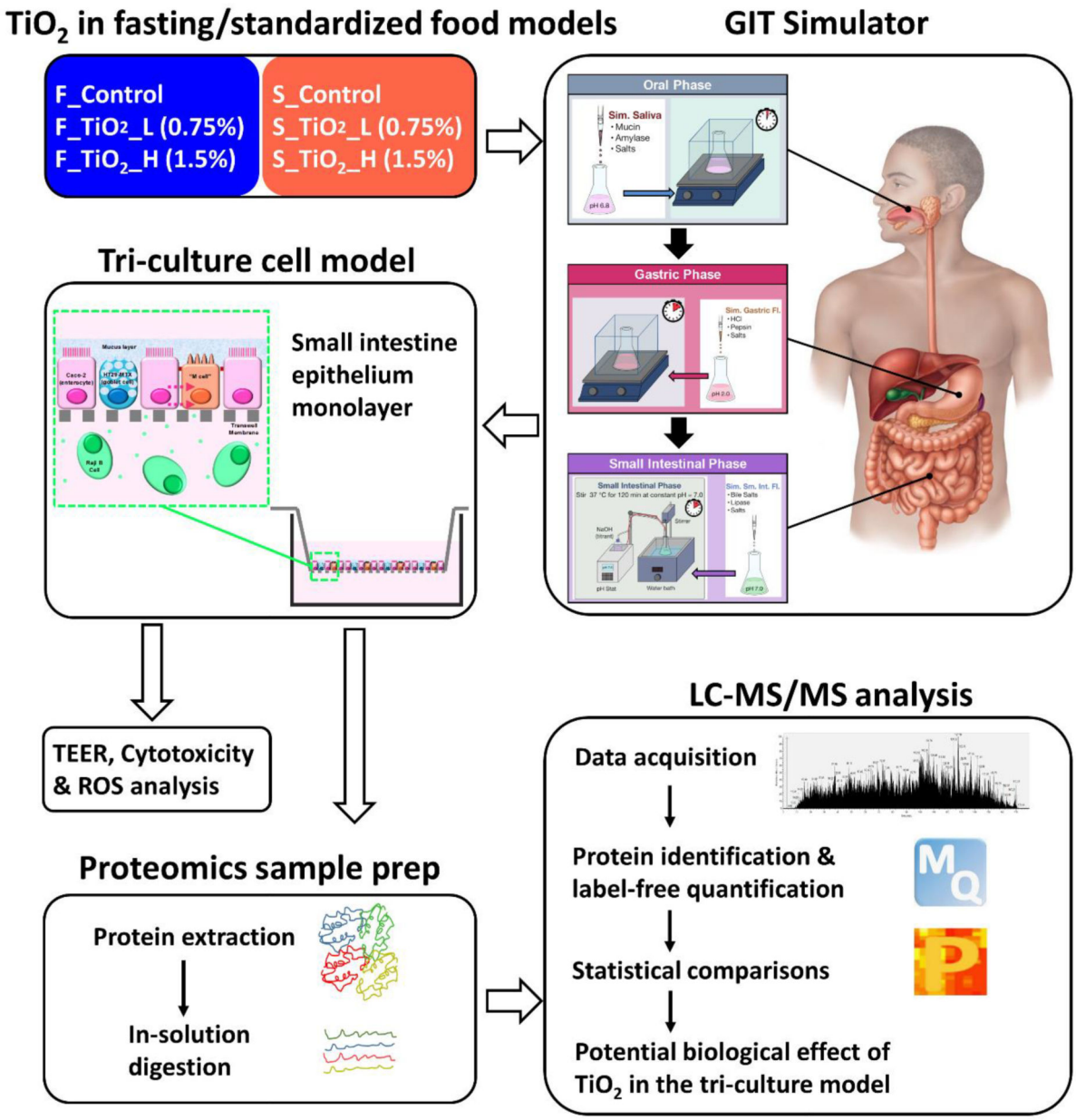

Figure 1.
Schematic diagram of the study design.

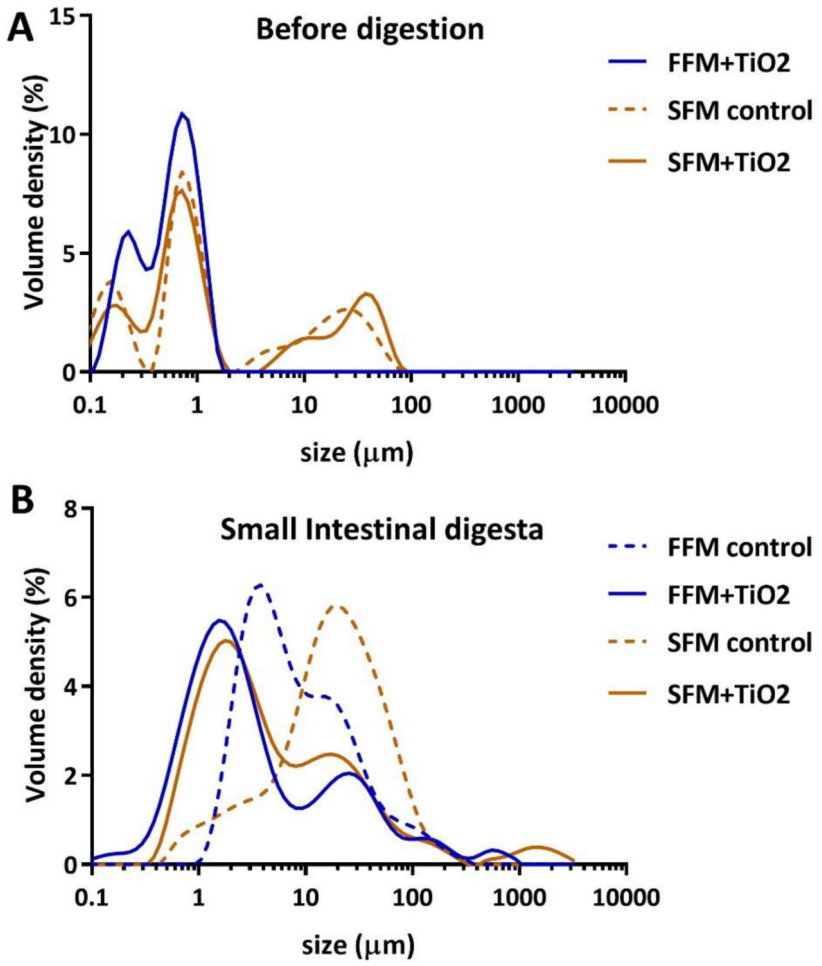

Figure 2.

Size distributions of particles before digestion and in small intestinal phase digesta. (A) Volume density (%) of particle diameter distributions for TiO_2 in FFM (fasting food model, phosphate buffer), SFM (standardized food model) control, and TiO_2 in SFM. (B) Volume density (%) of particle diameter distributions for small intestinal phase digesta of FFM control, TiO_2 in FFM, SFM control, and TiO_2 in SFM.

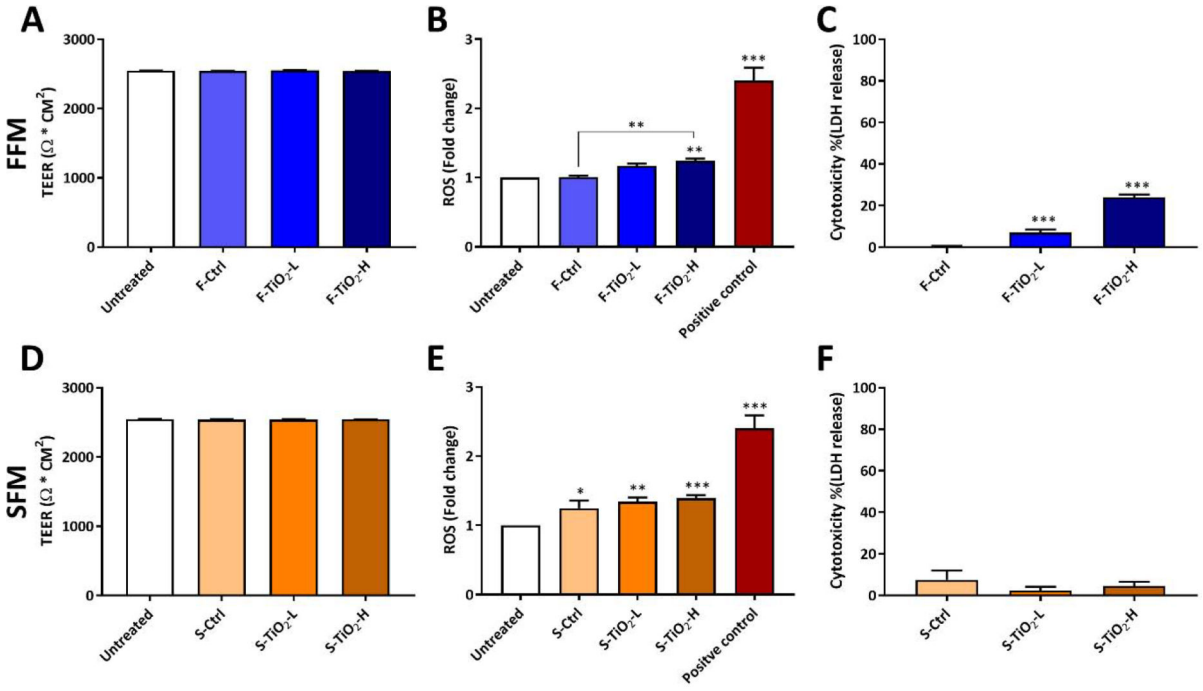

Figure 3.

In vitro toxicity of food-grade TiO_2 in fasting food model (A, B and C) and in standardized food model (D, E and F). TEER measurements after 24 h exposures to digesta from simulated digestion (A and D). ROS generation (fold change from untreated cells) following 6 h exposure to digesta from simulated digestion (B and E). Cytotoxicity (LDH assay) following 24 h exposure to digesta from simulated digestion (C and F). Error bars represent ±SD, *=p<0.05, **=p<0.01, ***=p<0.001.

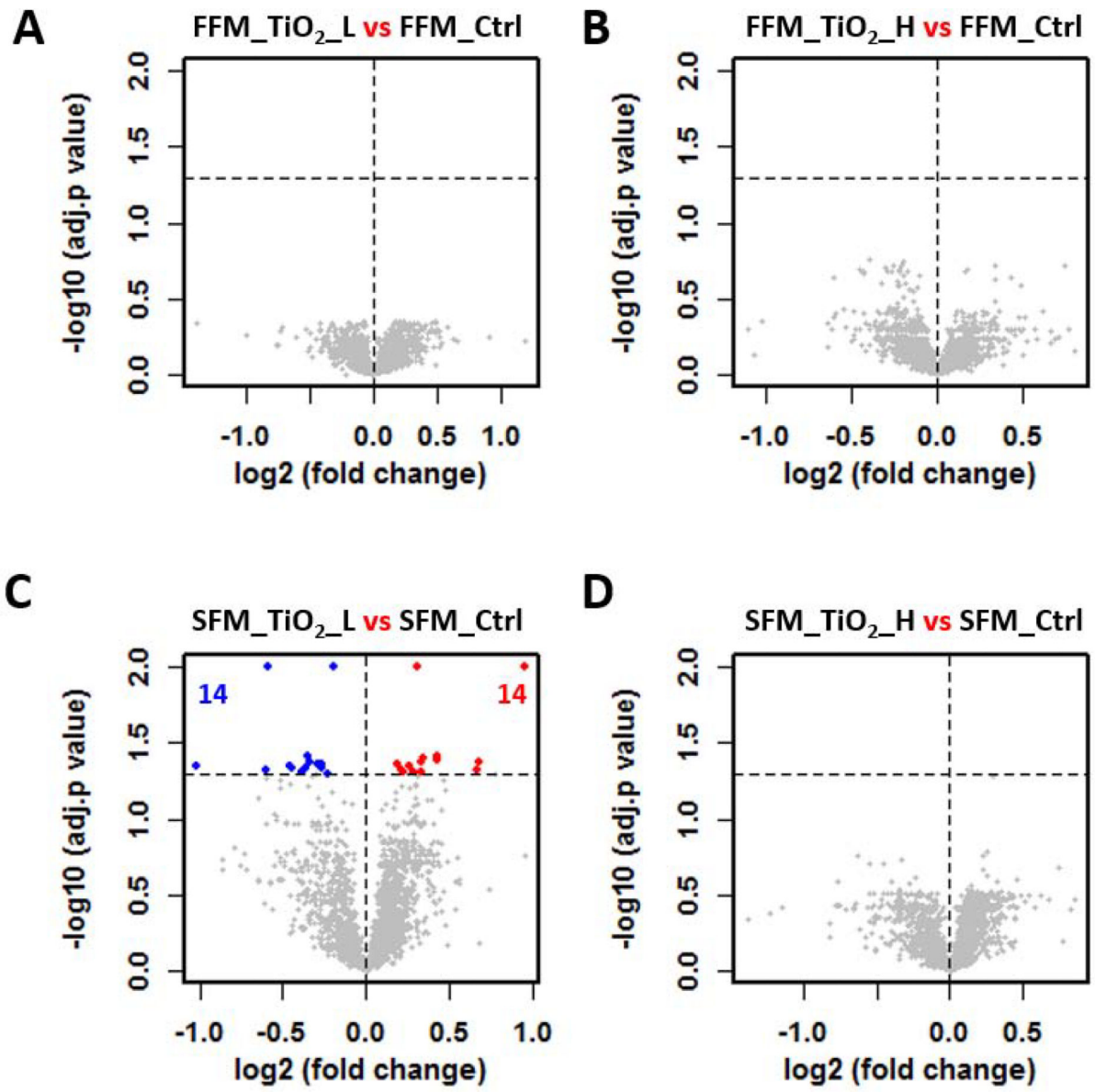

Figure 4.

TiO_2 induce little to no impact on the cellular proteome of the triculture system. Volcano plots were used to show the proteome difference involving four TiO_2 effect comparisons (A-D). Abbreviation scheme of comparing groups: food matrix (F for fasting and S for standard), followed by treatment (TiO_2_L and TiO_2_H for low and high dose of TiO_2 treatment, respectively, and Ctrl for the controls). x axis: the extent of fold change in protein intensity (in log2 scale); y axis: the level of statistical significance of the comparisons (-log adjusted p value). Red and blue dots represent significantly down- and up-regulated proteins, respectively. Grey dots represent non-significant regulated proteins. Black dotted horizontal line at y = 1.3, the cutoff to define significant proteins. The number of significantly down- and up-regulated proteins were shown in blue and red, respectively.

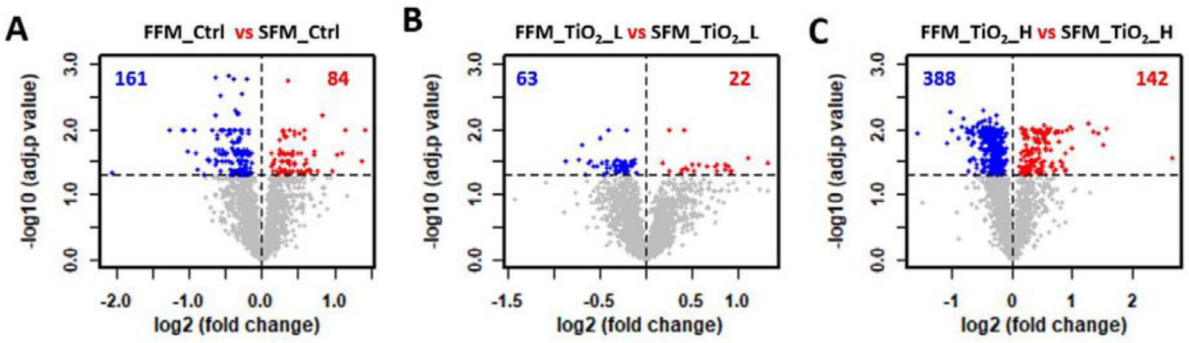

Figure 5.

Differential proteomes associated with food matrices. Volcano plots were used to show the proteome difference involving three food matrix effect comparisons (A-C).

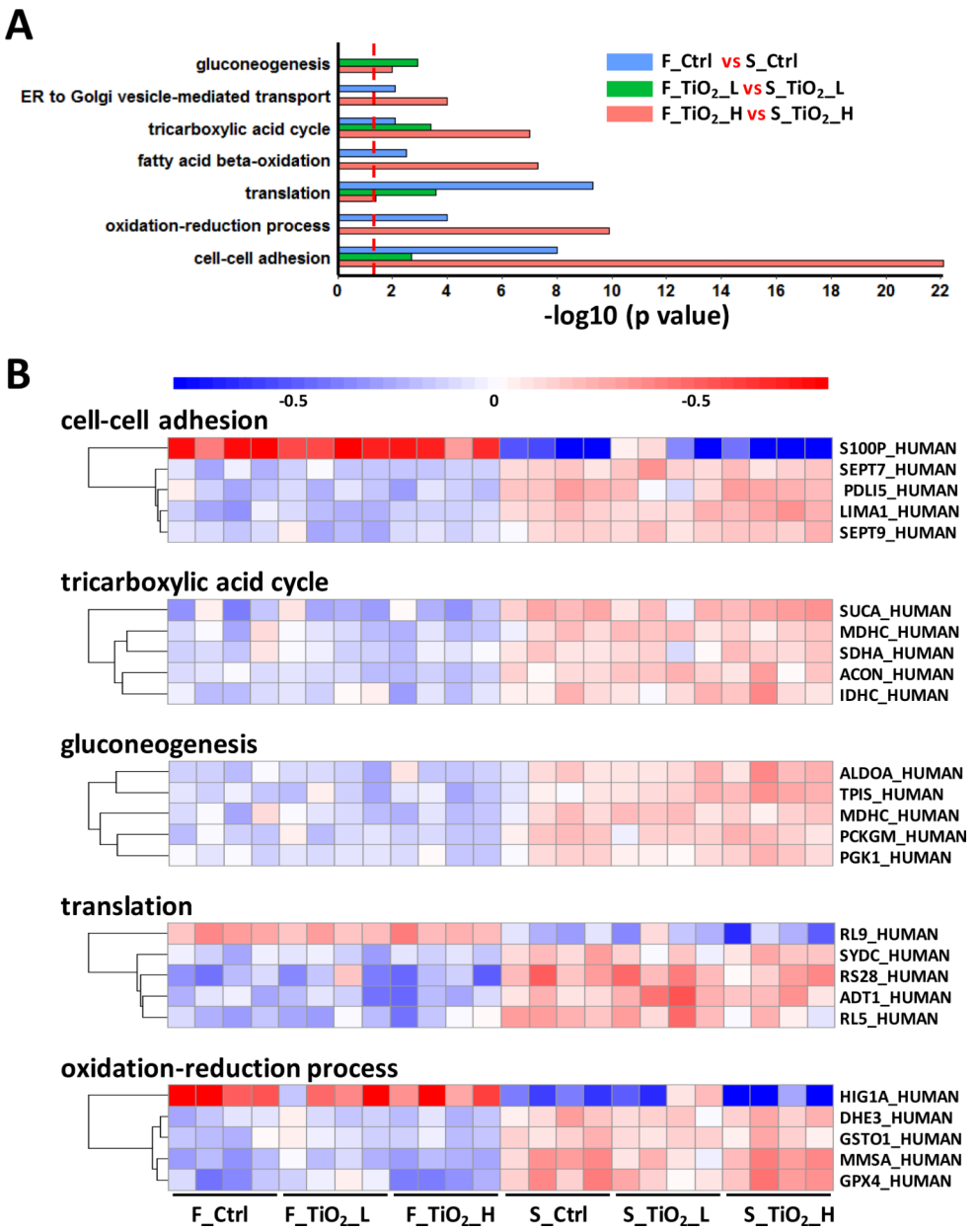

Figure 6.

Pathways and proteins in response to different food matrices. (A) Biological processes enriched from three food matrix effect comparisons. Significant proteins from each comparison were subjected to gene ontology enrichment, and the figure illustrated biological processes ($p < 0.01$) found from at least two out of the three comparisons. (B) Protein abundance changes in selected biological processes. Significant proteins in each biological process were subjected to t test between the two food matrix groups, and proteins with top 5 smallest p values were selected for plotting.

Table 1.

Colloidal characterization of TiO_2 (E171) before digestion and in small intestinal phase digesta.

	Sample	ζ (mV)	D[3,2] (μm)	D[4,3] (μm)	Dv10 (μm)	Dv50 (μm)	Dv90 (μm)
Before digestion	FFM control	-	-	-	-	-	-
	FFM+TiO_2	−40.5 ± 0.5	0.14 ± 0.01	0.60 ± 0.01	0.19 ± 0.01	0.57 ± 0.01	1.07 ± 0.01
	SFM control	−44.3 ± 1.7	0.46 ± 0.01	9.39 ± 1.81	0.145 ± 0.01	0.87 ± 0.01	29.9 ± 2.3
	SFM+TiO_2	−44.0 ± 0.6	0.52 ± 0.01	9.89 ± 0.05	0.18 ± 0.01	0.83 ± 0.01	37.5 ± 0.4
Small intestinal digesta	FFM control	−20.9 ± 0.7	5.01 ± 0.21	16.7 ± 1.7	2.27 ± 0.05	6.44 ± 0.42	37.3 ± 4.1
	FFM+TiO_2	−20.9 ± 0.2	1.46 ± 0.05	35.8 ± 9.6	0.66 ± 0.01	2.32 ± 0.01	42.5 ± 2.4
	SFM control	−33.2 ± 0.9	6.73 ± 0.02	15.9 ± 12.7	2.60 ± 0.01	18.5 ± 0.4	68.4 ± 3.5
	SFM+TiO_2	−27.6 ± 0.8	2.29 ± 0.07	42.2 ± 29.8	0.91 ± 0.01	3.44 ± 0.20	43.9 ± 10.6